SVM Multi-class Classification Method for Device Identification Using Eye Diagram Parameters

Jian Yuan[1,2(✉)] and Aiqun Hu[1]

[1] School of Cyber Science and Engineering, Southeast University, Nanjing, People's Republic of China
{yuanj,aqhu}@seu.edu.cn

[2] Research Center of Hengtong Information Security, Suzhou, People's Republic of China

Abstract. In this paper, we investigate the problem of identification of RS-485 devices. The proposed method utilizes their physical layer features in terms of time-domain overlapping traces. The first step is the acquisition of the physical layer waveform with an oscilloscope. The waveform is then preprocessed, a pulse shaping filter is applied, and the eye diagram is generated. These eye diagram parameters are estimated and stored as datasets. Then, the datasets are divided into two conventional categories. The first one is defined as the training set for deriving key parameters, the second one is used as the test set to verify the proposed algorithm. The eye diagram parameters of the test set are used for training, and the parameters of multi-class the supporting vector machine (SVM) are obtained. The data from the testing set is used to classify the devices. The results of the classification are used for device identification. Our experimental results show that classification accuracies of RS-485 devices can be higher than 88%, which indicate that our proposed method is practical and thus has a potential to be used in a number of applications including industrial Internet of Things (IoT) device identifications.

Keywords: device identification · eye diagram · supporting vector machine · physical layer security

1 Introduction

Identification and authentication are two important security functions. Identification is the capability to uniquely identify an entity (e.g., user, system or application) among other entities. Authentication is the capability to prove that an entity (e.g., user, system or application) is what it claims to be. Identification and authentication is extensively used in ensuring the security of Information and Communication Technologies (ICT) for the access and provision of services. For example, it is critical to distinguish between legitimate users (who are paying for a service) from other users (who may use the same services in an illegal way). Identification and authentication can be based on three

X. Chen et al. (Eds.): IoTaaS 2023, LNICST 585, pp. 225–238, 2025.
https://doi.org/10.1007/978-3-031-70507-6_17

main factors: information that an entity knows (such as a password), something that entity has (a smartcard) or something the entity is (biometric features). Identification and authentication can be based on each of these elements or a combination of these elements in the so-called multi-factor authentication, which is usually stronger than Identification /authentication based on a single element. Each of these elements has its own advantages/disadvantages as it is well known in literature [1].

There are three main physical layer-based device identification methods: measuring received signal strength, channel state information, and device characteristics [2].

The received signal strength is mainly affected by channel characteristics, physical media and other factors. Some possible causes may include the distance and channel conditions. The distance between the transmitter to the receiver varies from 10 m to 10 km. The channel distortion may be introduced by the hardware circuits, inter-symbol interference (ISI), and copper line materials [3].

If we only measure the strength of the received signal, the channel features can not be used to distinguish the devices, because the strength dynamic values are not adequately stable [4]. Channel State Information (CSI) can separate the multipath components, so it can provide a more fine-grained fingerprint based on the state of the medium. For example, in the case of Wi-Fi networks, the presence of multiple subcarriers makes CSI-based device identification more characteristic [5].

The third method of physical layer identification is to use device characteristics (such as hardware manufacturing defects) for identification. Such defects in hardware will cause offsets in transient or steady-state signals during signal transmission, thus generating device fingerprints [6]. The classification and identification of wireless devices using device fingerprints is mainly divided into three steps: (a) collect the signals emitted by the device to be identified; (b) extract appropriate signal characteristics; (c) use signal characteristics to create device fingerprints and classify device fingerprints. By extracting and analyzing these device fingerprints, the purpose of device classification can be achieved [7–9].

In general, the device fingerprint should have the following characteristics [10–12]. (a) Uniqueness: No two devices can have the same fingerprint. (b) Persistence: The device fingerprint obtained should remain unchanged for a long time. (c) Collectability: The signal emitted by the device to be identified can be captured by existing acquisition equipment. (d) Robustness: The characteristics should be unaffected by environmental factors and channel environment.

Eye diagram is a kind of graph which is presented by overlapping signals gradually accumulated on oscilloscope [13–15]. It contains rich damage information, which can completely reflect the performance characteristics of optical signal, qualitatively reflect the influence of various damage on signal quality, and then reflect the pros and cons of optical communication system [16]. From the eye diagram, we can not only obtain the modulation format information, but also estimate the signal quality indicators such as height, width and so on [11]. Therefore, eye diagrams have long been the core and first choice for signal integrity embodiment. In this paper, the eye diagram of the signal is used as the analysis object to extract the device features for training and identification of the device [17].

In order to quickly and effectively judge and evaluate the integrity of the time domain waveforms, some characteristics must be derived from the obtained eye diagram image, then the relevant parameters are defined according to several key positions of the eye diagram [18]. Through the judgment and estimation of these key parameters, the performance of the optical network system is effectively measured. There are many eye diagram parameters related to the system performance change, such as low level, high level, eye height, eye width, eye amplitude, extinction ratio, eye cross ratio, average power, Q factor, jitter, etc. These parameters can be used for feature extraction to identify different devices.

The organization of the rest of this paper is as follows. In Sect. 2, we discuss the standard RS-485 protocols and some common features of hardware devices. Next, in Sect. 3, the multiclass SVM theory is reviewed. Furthermore, the experimental findings and results are shown and explained in more detail in Sect. 4.

2 Analysis of an RS-485 Device's Eye Diagram

2.1 The RS-485 Bus Overview

The traditional RS-485 bus technology plays a crucial role in current industrial production due to its numerous advantages. Its key characteristics are as follows:

The RS-485 bus network utilizes differential signal technology at the physical layer. The voltage difference between twisted pair lines represents high-level signal logic, ranging from positive 2 V to positive 6 V, while the voltage difference representing low-level signal logic 0 ranges from negative 2 V to negative 6 V. The specified signal voltage by the RS-485 bus interface standard is relatively low, reducing the complexity in designing and producing bus driver chips. Moreover, the level specified by the RS-485 bus standard is compatible with TTL level, facilitating interconnection with TTL circuits (see Fig. 1).

Fig. 1. RS-485 Specified Minimum Bus Signal Levels

In the physical layer of the RS-485 bus, a balanced driver and differential receiver solution are employed. This means that when transmitting data using RS-485 bus technology, signals are modulated into symmetric signals sent through two lines (balanced transmission). If a single line is used for transmission (with a reference level), it is referred to as unbalanced transmission. On the receiving end of RS-485 bus technology, symmetric reception (balanced reception) is utilized; however, if asymmetric reception occurs (single-line reception corresponding to one reference level), it is considered unbalanced reception. The physical layer technology of RS-485 provides excellent resistance against common mode interference or external noise (see Fig. 2).

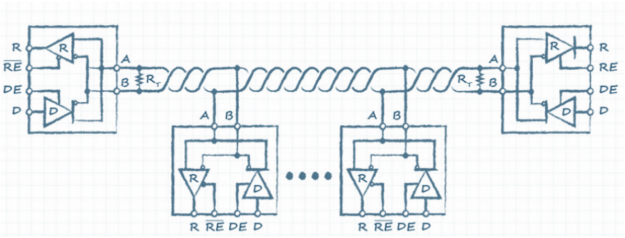

Fig. 2. Typical RS-485 network topology

2.2 Line Coding

The RS-485 bus utilizes digital data for signal transmission, employing direct encoding of binary digital data through the use of digital signals. The coding methods commonly employed include Non Return To Zero (NRZ) coding and Non Return to Zero Inverse (NRZI) coding. NRZ coding represents transmitted data using high and low signal levels, with high level representing data 1 and low level representing data 0. NRZI coding represents transmitted data based on whether there is a transition at the start of each bit; no transition indicates data 1, while a transition indicates data 0. Non-return-to-zero coding is often used in short-range communication due to its simplicity in implementation. However, it can result in DC drift due to an unequal distribution of zeros and ones when continuously transmitting either all zeros or all ones, thereby affecting stable signal transmission.

In our study, RS-485 Communication channel model is shown in Fig. 3. At the transmitter, binary data is encapsulated into an RS-485 protocol frame and subsequently encoded by hardware before being transmitted through the channel. Upon acquisition of the time-domain waveform on the channel, an eye diagram can be generated for further usage. At the receiver, decoding via hardware yields output in binary format.

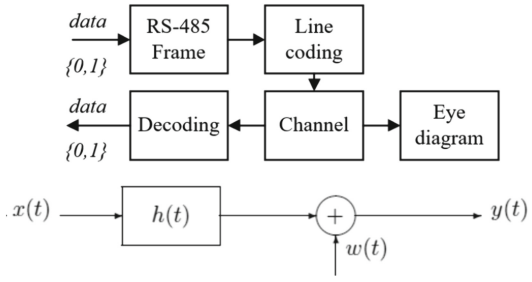

Fig. 3. RS-485 Communication channel model

2.3 Wireline Communication Model

When an electric signal is transmitted over a channel, it will be definitely contaminated. This may due to various signal transmission path imperfections. The reasons of signal

distortion are now analyzed as follows. The received waveform is defined as

$$y(t) = x(t) * h(t) + w(t) \tag{1}$$

where $w(t)$ represents several linear or non-linear noise processes.

1) **Channel noises**
   The simplest noise is the additive white Gaussian noise (AWGN). This can be used for mathematical modelling various physical transmission path. However, the RS-485 wireline channel may also introduce other types of noises, such as amplifier nonlinearities caused by hardware impairments.
2) **Linear Distortion**
   We shall first consider linear time-invariant channels. Signal distortion can be caused over such a channel by nonideal characteristics of magnitude distortion, phase distortion, or both.
   We can identify the effects these nonidealities will have on a pulse $h(t)$ transmitted through such a channel.
3) **Distortion Caused by Channel Nonlinearities**
   The linear channel is applicable only to weak signals, while for strong signals, the significance of nonlinearity becomes more prominent. The nonlinear channel can be modeled as follows: we consider a memoryless simple scenario where both the input h and output y are governed by a set of nonlinear equations.

$$y = f(h) \tag{2}$$

After expansion, this equation can be express as

$$y(t) = a_o + a_1 h(t) + a_2 h^2 h^2 + \cdots \tag{3}$$

In a digital communication system, linear and nonlinear distortions have significantly different impacts on the signal. Linear distortion can cause interference between signals in the same frequency band, while nonlinear distortion can lead to interference between signals in different frequency bands.

2.4 Features of Eye Diagram

In order to efficiently and effectively assess the signal quality based on the shape characteristics of the generated eye image, relevant parameters are defined for key positions within the eye image. The performance is accurately evaluated by analyzing and estimating these key parameters. There exist numerous Eye diagram parameters that are associated with changes in system performance, including "Zero"/"One" Level, Eye Height, Eye Width, Eye Amplitude, among others (see Fig. 4).

The following key eye diagram parameter indicators are briefly introduced:

(1) "0" level and "1" level: In the eye diagram, these levels represent the logic 0 and logic 1 voltage of the received signal. The middle value of the eye diagram is selected as a reference point (20% of the signal peak value), and by projecting it vertically in the eye diagram, a histogram is obtained. The median value of this projection represents the "0" and "1" levels.

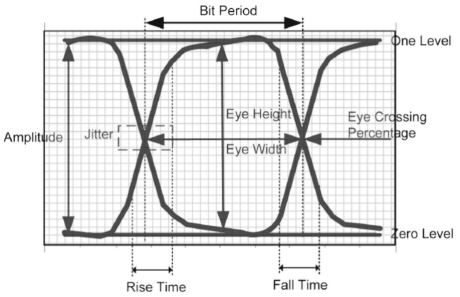

Fig. 4. Typical Eye Diagram Measurements

(2) Amplitude of eye: It signifies the difference between mean values of signal distribution represented by logic voltage "1" and logic voltage "0". Similar to determining the "0"/"1" level in an actual measurement, it involves calculating differences within a 20% distribution area near the middle position of an eye diagram.
(3) Height of eye: This indicates how open or closed an eye is in terms of vertical direction at its midpoint. While similar to measuring amplitude, it specifically focuses on capturing maximum differences within an eye diagram. The height reflects both noise-induced distortion in signals and serves as a measurement for signal-to-noise ratio.

These parameters can be used for feature extraction to identify different devices.

3 An Introduction to LS-SVM Algorithm

3.1 Introduction to Support Vector Machines

SVM is first proposed to distinguish binary classes. Then, it is applied to solve functional regression problem and multi-class classification problems. Although SVM algorithms are suitable for solving binary classification problems, a large number of multi-class classification problems in practical applications are also needed to solve by using extended SVM algorithms. At present, there are the following commonly used methods:

(1) One-to-many method. The idea is to treat the samples from one class as one class and the samples from the remaining classes as another class, making it a two-class classification problem. Then, the above steps are repeated for the remaining samples. This approach requires constructing K-SVM models, where K represents the amount of classes to be classified. However, this scheme usually needs a large number of training samples.
(2) One-to-one method. The multiclass classification problems involve considering only two classes at a time, resulting in the utilization of the SVM model for each pair of classes. Consequently, K(K-1)/2 SVM models are designed in total. Generally, this approach necessitates constructing multiple binary classifiers and subsequently comparing every pair of classes, thereby leading to a significant increase in computational complexity.

(3) Decision tree method. This method involves combining binary classification decisions to create a multi-class recognizer. However, one drawback of this approach is that if a classification error occurs at any node, it will propagate and impact the overall recognition accuracy.

3.2 Application of Support Vector Machine in Classification Problem

Firstly, let us consider the linearly separable case, and suppose there are linearly separable training samples:

$$(x_i y_i), x_i \in R^n, y_i \in \{+1, -1\}, i = 1, \ldots, l \tag{4}$$

The objective of the separation problem is to identify a hyperplane that can effectively and completely separate the two classes of samples. On one hand, the optimal separating hyperplane should accurately classify the samples into their respective classes, on the other hand, it should maximize the distance between the closest data points from each class and the hyperplane. This distance is referred to as the maximum classification margin.

Finally, the discriminant function is obtained as

$$f(x) = \operatorname{sgn}\left(\sum_{i=1}^{l} \alpha_i y_i K(x_i, x) + b\right) \tag{5}$$

where $\alpha_i \geq 0, i = 1, \cdots, l$.

In general, the solution to the above-mentioned problem can be found, since most values of α_i will be zero. The samples corresponding to the non-zero a will be the Supporting Vector (SV).

3.3 Multiple Classification Algorithm

The one-class classification method under linear programming can be extended to the multiple classification case in the following. The proposed method involves the classification of each class of samples, followed by the derivation of the decision function $f(x)$ for binary classification. Then the sample to be tested is input into each decision function, and the class to which the point belongs is determined according to the maximum value of the decision function. The specific algorithm is described as follows:

Let the training samples be:

$$\{(x_1, y_1), \cdots, (x_i, y_i)\} \subset R^n \times R \tag{6}$$

where n is the dimension of the input sample, $y_i \in \{1, 2, \cdots, M\}$, and M is the number of categories. The samples are divided into M classes, and each class is written as follows.

$$\{(x_1^{(m)}, y_1^{(m)}), \cdots, (x_{l_m}^{(m)}, y_{l_m}^{(m)}), m = 1, \cdots, M\} \tag{7}$$

where $x_1^{(m)}$ and $y_1^{(m)}$ represents training samples of the m-th class, and $l_1 + \cdots + l_M = l$. Then we can formulate a linear programming problem as follows:

$$\min\left\{C\sum_{m=1}^{M}\sum_{i=1}^{l}\xi_{mi} + \rho\right\} \tag{8}$$

The constraint here is

$$\sum_{j=1}^{l_m}\alpha_j^{(m)}k(x_j^{(m)}, x_i^{(m)}) \geq p - \xi_{mi}, i = 1, \cdots, l_m \tag{9}$$

$$\sum_{j=1}^{l_m}\alpha_j^{(m)} = 1, \tag{10}$$

$$\alpha_i^{(m)}, \xi_{mi} \geq 0, i = 1, \cdots, l_s \tag{11}$$

Solving this linear program, M decision functions can be obtained

$$f_m(x) = \sum_{j=1}^{l_m}\alpha_j^{(m)}k(x_j^{(m)}, x) \tag{12}$$

Given a sample z to be identified, calculate $\gamma_i = f_i(z), i = 1, \cdots, M$, by comparing their values, the largest γ_k can be obtained. This indicates that z classified as the k-th class.

4 Experimental Results

4.1 RS-485 Devices for Different Sensors

We assume that there are 5 sensors in the industrial site, each sensor collects different types of field data, and then data transmission is carried out through the RS-485 bus. At the same time, these devices use the same hardware scheme including chips, resistors, capacitors and inductors. However, the material and length of the copper cable connecting the device are different (see Fig. 5).

These types of sensors include temperature, humidity, illuminance, vibration, pressure, acceleration, distance, and gases (see Table 1).

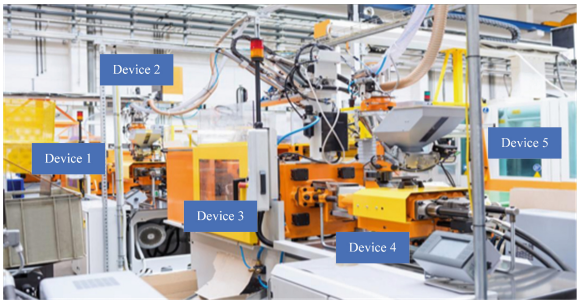

Fig. 5. RS-485 devices in a factory

Table 1. RS-485 devices of the same vendor.

Device Number	Sensor type
RS-485 Device 1	Temperature
RS-485 Device 2	Humidity
RS-485 Device 3	Illuminance
RS-485 Device 4	Vibration
RS-485 Device 5	Pressure

4.2 Overall Flow Diagram of RS-485 Device Classification

The overall process of device identification is shown in the following figure. The first step is the acquisition of the physical layer waveform with an oscilloscope. The waveform is then preprocessed, a pulse shaping filter is applied, and the eye diagram is generated. The eye diagram datasets are categorized into two groups, with 60% of the data allocated for training purposes and the remaining 40% designated as the test set. The eye diagram of the test set is used for training, and the parameters of the SVM are obtained. The data from the test set is used to classify the devices. The result of the classification is used for device fingerprint extraction (see Fig. 6).

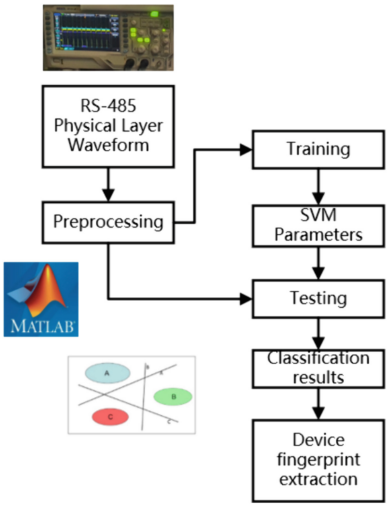

Fig. 6. RS-485 device fingerprint extraction

4.3 Physical Signal Acquisition by an Oscilloscope

Most of the oscilloscopes contain simple Math functions. Using this functionality, the second channel can be subtracted from the first channel.

The subtraction result must be inverted. After this result should look more correct. The noise level was decreased.

The RS-485 waveform can be saved as a *.csv file using USB portable disk, and then the raw datum in this file can be preprocessed by MATLAB.

4.4 Eye Diagram Generation Using MATLAB

(1) Raised Cosine Pulse

The Nyquist criterion states that an impulse response of a filter must satisfy certain conditions in order to eliminate ISI. In practical engineering, where the channel transmission inevitably introduces signal distortion, an equalizer can be employed at the receiver to mitigate ISI. This aspect will be elaborated further due to the uncontrollable nature of channel characteristics, whereby controlling both transmit and receive filters allows for manipulation of the overall impulse response of the transmission system. Consequently, the entire transfer function H(f) can be approximated as a product of transmitter and receiver filter functions. An efficient end-to-end transfer function, H(f), is typically achieved by employing filters with H(f) as their transfer functions at both ends. Such filters exhibit a frequency domain characteristic known as square-root raised cosine roll-off property; this property is demonstrated when cascading two square root raised cosine roll-off filters at both transmitter and receiver stages in the frequency domain (see Fig. 7).

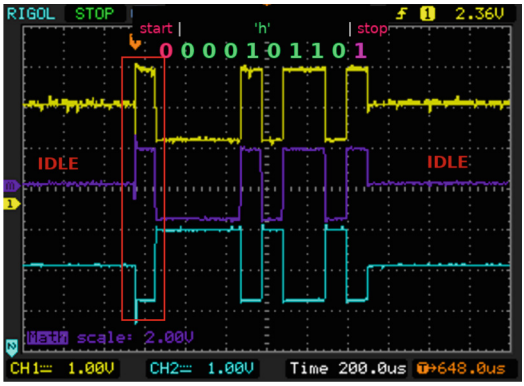

Fig. 7. Encoder output driven by differential driver and reconstructed by receiver

(2) Eye Diagram of RS-485 Devices

In the present study, we conduct a time-domain eye diagram test on the 10 Mbps signal. The test is performed using an oscilloscope and a 100 m twisted pair cable. Here's the procedure for conducting the test: an instrument is connected to one end of the bus, and random data is transmitted through the bus. The random data is generated by an FPGA at a rate of 10 Mbps, with consecutive sequences of 0 s or 1 s not exceeding a length of 7. This process is repeated continuously. The other end of the bus is connected to an oscilloscope, which measures and analyzes the eye diagram of the bus signal. Matching

resistors are configured at both ends of the bus, allowing us to assess signal quality by adjusting their values. Then the datum are stored in a USB disk. Finally, these datum are pre-processed in MATLAB (see Fig. 8).

4.5 Feature Extraction Using Eye Diagram Parameters

The eye diagram encompasses numerous parameters, among which we have adopted the transverse time parameter and the longitudinal amplitude parameter. Lateral time parameters include eye width, rise time, fall time, etc., while longitudinal amplitude parameters encompass "0" Level, "1" level, Mean Level, Eye amplitude, Eye Height, etc. (see Fig. 8).

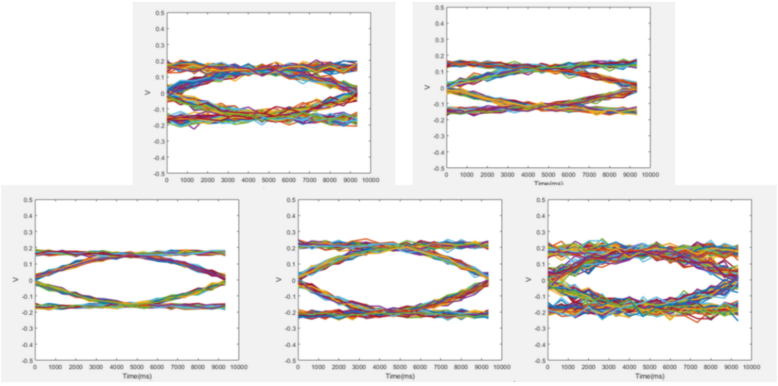

Fig. 8. Eye diagrams of RS-485 devices

The fundamental longitudinal eye diagram parameters are defined by the "0" level and the "1" level. Specifically speaking, in a complete eye diagram, data points located within the central 20% of the diagram are projected onto the vertical axis to form a histogram. The center values of this histogram represent levels "1" and "0", respectively.

Another crucial parameter in longitudinal eye plots is eye height. It signifies the vertical opening within an eye diagram and reflects interference from noise. A larger eye height indicates less distortion in signal quality with respect to amplitude.

Eye width denotes the horizontal opening inside an eye diagram. By dividing two adjacent intersections of the diagram into two sets and considering data points within these sets as Gaussian distributions as well.

Based on both eye width and eye amplitude measurements, one can calculate rise time and fall time accordingly. These times refer to transitions from a 10% amplitude to a 90% amplitude (see Table 2).

Table 2. Eye diagram parameter used for devices feature.

Device Feature 1	Device Feature 2	Device Feature 3	Device Feature 4	Device Feature 5	Device Feature 6
Zero Level	One Level	Eye Height	Eye Width	Eye Rise Time	Eye Fall Time

4.6 Data Preprocessing Using Python

(1) Standardisation

The purpose of normalization is to ensure that the mean is centered at zero and the standard deviation is scaled to one by resizing the data. The formula can be expressed as follows:

$$x_{std} = \frac{x - mean(x)}{std(x)} \tag{13}$$

(2) Max-Min Normalization

Another commonly employed technique for data preprocessing is max-min normalization, which transforms all sample values into a range between 0 and 1. For each feature, the minimum value is mapped to 0 while the maximum value is mapped to 1. The general formula for this process can be stated as follows:

$$x_{norm} = \frac{x - \min(x)}{\max(x) - \min(x)} \tag{14}$$

4.7 Test Results

In this experiment, we collected a total of 250 samples, 50 samples for each device. We split these 250 samples into training and test sets. The training set is 60% and the test set is 30%. General data in the test set for cross-validation.

The classification accuracy can reach 90%, and the classification performance is good, which proves that the RS-485 device fingerprint extraction technology based on eye diagram parameters and support vector machine is feasible. The confusion matrix is shown in Table 3.

Table 3. Confusion matrix results.

Device 1	**0.90**	0.06	0.04	0.00	0.00
Device 2	0.00	**0.92**	0.03	0.05	0.00
Device 3	0.00	0.00	**0.95**	0.03	0.02
Device 4	0.00	0.06	0.04	**0.88**	0.02
Device 5	0.00	0.00	0.00	0.00	**0.93**
	RS-485 Device 1	RS-485 Device 2	RS-485 Device 3	RS-485 Device 4	RS-485 Device 5

5 Conclusions

In this paper, we study the problem of physical layer feature extraction for 485-bus devices. We first analyze the signal characteristics of 485 bus device, and find that its eye diagram parameters can be used to do feature extraction. Next, we introduce the algorithm of support vector machine. In the experiment section, we detail the steps of the 485-bus device physical signal acquisition, eye diagram generation method, feature extraction and data preprocessing. The experimental results indicate that the correct classification rate of most devices is more than 90%, which means that different devices can be recognized basically. In future work, we will further test more devices and plan to combine eye map features and sensor data features to further improve the accuracy.

References

1. Yener, A., Ulukus, S.: Wireless physical-layer security: Lessons learned from information theory. Proc. IEEE **103**(10), 1814–1825 (2015)
2. Pappu, R., Recht, B., Taylor, J., Gershenfeld, N.: Physical one-way functions. Science **297**(5589), 2026–2030 (2002)
3. Rührmair, U., Busch, H., Katzenbeisser, S.: Strong PUFs: models, constructions, and security proofs. Towards Hardware-Intrinsic Security: Foundations and Practice, 79-96 (2010)
4. Kori, B., Maubach, S., Kevenaar, T., Tuyls, P.: Information-theoretic analysis of capacitive physical unclonable functions. J. Appl. Phys. **100**(2), 024902–024911 (2006)
5. Baldini, G., Giuliani, R., Steri, G.: Physical layer authentication and identification of wireless devices using the synchro-squeezing transform. Appl. Sci. **8**(11), 2167 (2018)
6. Jiang, Y., Peng, L., Hu, A., Wang, S., Huang, Y., Zhang, L.: Physical layer identification of LoRa devices using constellation trace figure. EURASIP J. Wirel. Commun. Netw. **2019**(1), 273 (2019)
7. Peng, L., Zhang, J., Liu, M., Hu, A.: Deep learning based RF Fingerprint identification using differential constellation trace figure. IEEE Trans. Veh. Technol. **69**(1), 1091–1095 (2020)
8. Liu, M., Liao, G., Yang, Z., Song, H., Gong, F.: Electromagnetic signal classification based on deep sparse capsule networks. IEEE Access **2019**(7), 83974–83983 (2019)
9. J. Carbino T., A. Temple M., J. Bihl T.: Ethernet card discrimination using unintentional cable emissions and constellation-based Fingerprinting. In: International Conference on Computing, Networking and Communications (ICNC) 369–373 (2015)
10. Ometov, A., Bezzateev, S., Mäkitalo, N., Andreev, S., Mikkonen, T., Koucheryavy, Y.: Multi-factor authentication: A survey. Cryptography **2**(1), 1–4 (2018)
11. Masdari, M., Ahmadzadeh, S.: A survey and taxonomy of the authentication schemes in telecare medicine information systems. J. Netw. Comput. Appl. **87**, 1–19 (2017)
12. Mukherjee, A.: Physical-layer security in the internet of things: sensing and communication confidentiality under resource constraints. Proc. IEEE **103**(10), 1747–1761 (2015)
13. Chen, X., Li, J., Han, H., Ying, Y.: Improving the signal subtle feature extraction performance based on dual improved fractal box dimension eigenvectors. Royal Soc. Open Sci. **5**(5), 180087 (2018)
14. Li, J., Ying, Y., Lin, Y.: Verification and recognition of fractal characteristics of communication modulation signals. In: IEEE 2nd International Conference on Electronic Information and Communication Technology (ICEICT) (2019)
15. Tu, Y., Lin, Y., Wang, J., Kim, J.U.: Semi-supervised learning with generative adversarial networks on digital modulation classification. Comput. Mater. Cont. **55**(2), 243–254 (2018)

16. Han, H., Li, J., Chen, X.: The individual identification method of wireless device based on a robust dimensionality reduction model of hybrid feature information. Mob. Netw. Appl. **23**(4), 709–716 (2018)
17. Merchant, K., Revay, S., Stantchev, G., Nousain, B.: Deep learning for RF device Fingerprinting in cognitive communication networks. IEEE J. Select. Topics Signal Process. **12**(1), 160–167 (2018)
18. Yu, J., Hu, A., Li, G., Peng, L.: A robust RF Fingerprinting approach using multisampling convolutional neural network". IEEE Int. Things J. **6**(4), 6786–6799 (2019)